

Low energy Lorentz violation from high energy modified dispersion in inertial and circular motion

Jorma Louko* and Samuel D. Upton†

School of Mathematical Sciences, University of Nottingham,
Nottingham NG7 2RD, UK

Revised December 2017

Published in Phys. Rev. D **97**, 025008 (2018)

Abstract

We consider an Unruh-DeWitt detector in inertial and circular motion in Minkowski spacetime of arbitrary dimension, coupled to a quantised scalar field with the Lorentz-violating dispersion relation $\omega = |\mathbf{k}| f(|\mathbf{k}|/M_\star)$, where M_\star is the Lorentz-breaking scale. Assuming that f dips below unity somewhere, we show that an inertial detector experiences large low energy Lorentz violations in all spacetime dimensions greater than two, generalising previous results in four dimensions. For a detector in circular motion, we show that a similar low energy Lorentz violation occurs in three spacetime dimensions, and we lay the analytic groundwork for examining circular motion in all dimensions greater than three, generalising previous work by Stargen, Kajuri and Sriramkumar in four dimensions. The circular motion results may be relevant for the prospects of observing the circular motion Unruh effect in analogue laboratory systems.

1 Introduction

Many theories of quantum gravity suggest that a fundamental quantum description of spacetime induces violation of local Lorentz invariance in the effective low energy description of matter as a quantum field theory on a classical spacetime [1]. Constraining local Lorentz violations observationally provides hence a potential constraint on quantum theories of gravity. Despite the large disparity between experimentally accessible energy scales and the Planck scale, which is usually thought to characterise quantum gravity phenomena, such constraints can be nontrivial: in quantum field theory, it is possible for the effective low energy theory to bear unexpected imprints of the theory's high energy structure [2, 3].

*jorma.louko@nottingham.ac.uk

†eeysdu@exmail.nottingham.ac.uk

In this paper we consider a Lorentz-violating scalar field theory with the dispersion relation

$$\omega_{|\mathbf{k}|} = |\mathbf{k}|f(|\mathbf{k}|/M_\star) , \quad (1.1)$$

where we have set $c = \hbar = 1$, \mathbf{k} is the spatial momentum, $\omega_{|\mathbf{k}|}$ is the energy, M_\star is a positive constant of dimension energy, and the dimensionless function f satisfies $f(g) \rightarrow 1$ as $g \rightarrow 0$. For $|\mathbf{k}|/M_\star \rightarrow 0$, the dispersion relation becomes that of a relativistic massless field, $\omega_{|\mathbf{k}|} = |\mathbf{k}|$, and we may hence think of M_\star as the characteristic energy scale of Lorentz violation.

Crucially, we assume that f dips below unity somewhere. An example is the low energy sector of a scalar field quantised in the polymer quantisation framework [4, 5, 6, 7, 8, 9], motivated by loop quantum gravity [10, 11]. Similar dips occur also in condensed matter systems, including the roton minimum of Helium 3 [12].

In four-dimensional Minkowski spacetime, an inertial Unruh-DeWitt detector [13, 14] coupled to a quantum field with these properties was shown in [15] to be able to undergo spontaneous excitations, and it was shown in [16] that the detector experiences drastic Lorentz-violating excitations and de-excitations at arbitrarily low energies whenever the detector's speed in the preferred frame exceeds the critical value that equals the infimum of f . The purpose of the present paper is to generalise these observations in two ways.

First, we show that the inertial detector experiences a similarly drastic low energy Lorentz violation in Minkowski spacetimes of all dimensions greater than three, and a less drastic but still large low energy Lorentz violation in dimension three. In two dimensions, by contrast, the low energy Lorentz violation is suppressed by the factor $1/M_\star$, except for a finetuned resonance that occurs when the speed is very close to the critical value.

Second, we show analytically that a detector in uniform circular motion in three-dimensional Minkowski spacetime experiences a large low energy Lorentz violation above the same critical speed as in inertial motion, and we exhibit numerical results about the detailed form of these violations.

We also perform the analytic groundwork for investigating circular motion in all dimensions above three, generalising the four-dimensional work in [17]. Generalising our three-dimensional circular motion analytic and numerical techniques to four dimensions and beyond would require an improved control of the generalised hypergeometric functions that appear, analytically in terms of uniform asymptotic expansions, and numerically in terms of accurate numerical evaluation in regimes where certain combinations of the parameters are large.

While we do not have in mind a concrete experimental setup, we anticipate the results to have relevance not just for constraining fundamental quantum theories of gravity but also for designing analogue spacetime laboratory experiments, where the effective spacetime dimensionality of the system is often different from four [18, 19, 20, 21, 22]. For a selection of experimentally-motivated analyses of circular motion, see [23, 24, 25, 26, 27, 28, 29].

We begin in Section 2 with a review of an Unruh-DeWitt detector coupled linearly to a scalar field with the modified dispersion relation (1.1), assuming the field to be in its Fock-like vacuum and the detector to be on a worldline on which the Fock-like vacuum appears stationary. We work within first-order perturbation theory, taking first

the limit of weak interaction and then the limit of long interaction time. Section 3 addresses inertial motion, Section 4 addresses circular motion in $2 + 1$ dimensions, and Section 5 addresses circular motion in dimensions $3 + 1$ and greater. Section 6 provides brief concluding remarks. The proof of Theorem 4.1, characterising the low energy limit of circular motion in $2 + 1$ dimensions, is deferred to the Appendix.

We use units in which $c = \hbar = 1$. Θ denotes the Heaviside theta-function,

$$\Theta(x) = \begin{cases} 1 & \text{for } x > 0, \\ 0 & \text{for } x \leq 0. \end{cases} \quad (1.2)$$

$\lceil \cdot \rceil$ denotes the ceiling function, $\lceil x \rceil =$ the smallest integer greater than or equal to x . $o(1)$ denotes a quantity that goes to zero in the limit under consideration.

2 Field and detector

In this section we set up the notation for the field and the detector with which the field is probed.

2.1 Field

We work in $(n + 1)$ -dimensional Minkowski spacetime, where $n = 1, 2, \dots$. We write the metric in the distinguished reference frame as

$$ds^2 = -dt^2 + d\mathbf{x}^2 = -dt^2 + (dx^1)^2 + \dots + (dx^n)^2. \quad (2.1)$$

We consider a scalar field ϕ with the dispersion relation (1.1), where \mathbf{k} is the spatial momentum, $\omega_{|\mathbf{k}|}$ is the energy, M_\star is a positive constant of dimension energy, and f is a dimensionless function of a non-negative dimensionless variable. We assume that f is smooth and positive-valued, and $f(g) \rightarrow 1$ as $g \rightarrow 0$.

We assume that ϕ admits a decomposition into spatial Fourier modes labelled by \mathbf{k} , such that each mode with spatial momentum $\mathbf{k} \neq \mathbf{0}$ is a harmonic oscillator with the angular frequency $\omega_{|\mathbf{k}|}$ (1.1), and the mode with $\mathbf{k} = \mathbf{0}$ is of measure zero and does not contribute to the decomposition. We include in the Fourier decomposition the density-of-states weight factor

$$\rho_{|\mathbf{k}|} = \frac{d(|\mathbf{k}|/M_\star)}{\sqrt{(2\pi)^n |\mathbf{k}|}}, \quad (2.2)$$

where d is a dimensionless complex-valued function of a non-negative dimensionless variable. We assume that d is smooth and nowhere vanishing, and $d(g) \rightarrow 1/\sqrt{2}$ as $g \rightarrow 0$. In the limit $M_\star \rightarrow \infty$ with fixed \mathbf{k} , we then have $\omega_{|\mathbf{k}|} \rightarrow |\mathbf{k}|$ and $\rho_{|\mathbf{k}|} \rightarrow (2(2\pi)^n |\mathbf{k}|)^{-1/2}$. The mode-by-mode $M_\star \rightarrow \infty$ limit of the field is hence the usual, Lorentz-invariant, massless scalar field.

If ϕ is viewed strictly as a scalar field, d and f are related by $d(g) = 1/\sqrt{2f(g)}$. We shall keep f and d independent, as this will also maintain applicability to situations

where the scalar field is an effective low energy limit of a more fundamental theory. One such situation is the low energy limit of the polymer quantised scalar field [7, 8, 9].

Finally, we introduce the crucial assumption that f dips below unity somewhere. For technical concreteness, we assume that the only stationary point of f is a global minimum at $g = g_c > 0$. Writing $f_c = f(g_c)$, we then have $0 < f_c < 1$. This is satisfied by the f that emerges from the low energy limit of the polymer quantised scalar field [7, 8, 9].

2.2 Detector

We probe the field by coupling it linearly to a spatially pointlike two-level quantum system known as the Unruh-DeWitt detector [13, 14]. This coupling models an atom interacting with the electromagnetic field when angular momentum interchange is negligible [30, 31], and it has been widely used to analyze motion effects in quantum field theory. We shall here just summarise the properties needed for the later sections. Text-book accounts can be found in [32, 33] and recent reviews in [34, 35, 36].

We consider a detector that moves on the prescribed worldline

$$\mathbf{x}(\tau) = (t(\tau), \mathbf{x}(\tau)) , \quad (2.3)$$

parametrised by the proper time τ . We set the field initially in its Fock vacuum.

In first-order perturbation theory, the probability of the detector to make a transition from the state with energy 0 to the state with energy E (which may be positive, negative or zero) is proportional to the response function,

$$\mathcal{F}(E) = \int d\tau d\tau' \chi(\tau) \chi(\tau') e^{-iE(\tau-\tau')} \mathcal{W}(\tau, \tau') , \quad (2.4)$$

where the switching function χ specifies how the interaction is turned on and off, \mathcal{W} is the pullback of the field's Wightman function to the detector's worldline,

$$\mathcal{W}(\tau, \tau') = G(t(\tau), \mathbf{x}(\tau); t(\tau'), \mathbf{x}(\tau')) , \quad (2.5)$$

and the Wightman function is given by

$$G(t, \mathbf{x}; t', \mathbf{x}') = \int d^n \mathbf{k} |\rho_{|\mathbf{k}|}|^2 e^{i\mathbf{k} \cdot (\mathbf{x} - \mathbf{x}') - i\omega_{|\mathbf{k}|}(t - t' - i\epsilon)} , \quad (2.6)$$

where the distributional character is encoded in the limit $\epsilon \rightarrow 0_+$. The constant of proportionality is quadratic in the coupling constant and depends on the internal structure of the detector, but it is independent of E and of the detector's trajectory, and we shall drop this constant from now on.

We consider detector trajectories for which the Fock vacuum is stationary, in the sense that $\mathcal{W}(\tau, \tau')$ depends on its arguments only through the difference $\tau - \tau'$. We may then convert \mathcal{F} into the transition rate per unit time by passing to the limit of adiabatic switching and factoring out the effective total duration of the detection. This procedure has significant conceptual and technical subtlety [35, 37, 38, 39], but the

outcome is that the transition rate is proportional to

$$\mathcal{F}_{\text{rate}}(E) = \int_{-\infty}^{\infty} ds e^{-iEs} \mathcal{W}(s, 0) . \quad (2.7)$$

In what follows we shall work with (2.7), dropping the “rate” subscript.

3 Inertial motion

In this section we consider a detector on the inertial worldline

$$\mathbf{x}(\tau) = (t(\tau), \mathbf{x}(\tau)) = (\tau \cosh \beta, 0, \dots, 0, \tau \sinh \beta) , \quad (3.1)$$

where $\beta \geq 0$ is the rapidity with respect to the distinguished inertial frame. For presentational simplicity we assume $\beta > 0$, but it can be verified that there is no discontinuity as $\beta \rightarrow 0$.

3.1 Spacetime dimension $2 + 1$ and greater

We start in spacetime dimensions $2 + 1$ and greater, so that $n \geq 2$. The case $n = 1$ will be addressed in subsection 3.3.

Inserting the trajectory (3.1) into (2.5), (2.6), and (2.7), we obtain

$$\begin{aligned} \mathcal{F}(E) &= \int_{-\infty}^{\infty} ds \int d^n \mathbf{k} |\rho_{|\mathbf{k}|}|^2 e^{-i(E + \omega_{|\mathbf{k}|} \cosh \beta - k_n \sinh \beta)s} \\ &= \Omega_{n-2} \int_{-\infty}^{\infty} ds \int_0^{\infty} dK K^{n-1} |\rho_K|^2 \int_0^{\pi} d\theta (\sin \theta)^{n-2} e^{-i(E + \omega_K \cosh \beta - K \sinh \beta \cos \theta)s} \\ &= 2\pi \Omega_{n-2} \int_0^{\infty} dK K^{n-1} |\rho_K|^2 \int_0^{\pi} d\theta (\sin \theta)^{n-2} \delta(E + \omega_K \cosh \beta - K \sinh \beta \cos \theta) \\ &= \frac{2\pi \Omega_{n-2}}{\sinh \beta} \int_0^{\infty} dK K^{n-2} |\rho_K|^2 \left(1 - \frac{(E + \omega_K \cosh \beta)^2}{K^2 \sinh^2 \beta} \right)^{(n-3)/2} \\ &\quad \times \Theta \left(1 - \frac{|E + \omega_K \cosh \beta|}{K \sinh \beta} \right) \\ &= \frac{2M_{\star}^{n-2}}{(4\pi)^{(n-1)/2} \Gamma\left(\frac{n-1}{2}\right) (\sinh \beta)^{n-2}} \\ &\quad \times \int_0^{\infty} dg |d(g)|^2 \Theta(g \sinh \beta - |(E/M_{\star}) + gf(g) \cosh \beta|) \\ &\quad \times \left(g^2 \sinh^2 \beta - [(E/M_{\star}) + gf(g) \cosh \beta]^2 \right)^{(n-3)/2} . \end{aligned} \quad (3.2)$$

The second equality follows by writing \mathbf{k} in spherical coordinates, such that $K = |\mathbf{k}|$ and $k_n = K \cos \theta$ with $\theta \in [0, \pi]$, and noting that the integral over the remaining $d - 2$

angles brings out the area of the unit sphere in Euclidean \mathbb{R}^{n-1} ,

$$\Omega_{n-2} = \frac{2\pi^{(n-1)/2}}{\Gamma(\frac{n-1}{2})} . \quad (3.3)$$

The next two equalities follow by performing the integrals over s and θ , respectively. In the final equality we have used (3.3) and introduced the new integration variable $g = K/M_\star$.

Recall [32] that the transition rate of the Lorentz-invariant massless scalar field can be obtained from the first line of (3.2) by setting $f(g) = 1$ and $d(g) = 1/\sqrt{2}$, with the result

$$\mathcal{F}_0^{in}(E) = \frac{(-E)^{n-2} \Theta(-E)}{2(4\pi)^{(n-2)/2} \Gamma(\frac{n}{2})} , \quad (3.4)$$

where the subscript 0 indicates the unmodified massless scalar field and the superscript *in* indicates inertial motion. Note that $\mathcal{F}_0^{in}(E)$ vanishes for $E > 0$: the Lorentz-invariant field induces no spontaneous excitations in the detector.

We wish to compare $\mathcal{F}(E)$ to $\mathcal{F}_0^{in}(E)$ in the low energy limit, $|E|/M_\star \ll 1$.

Suppose first that $n \geq 3$. The case $n = 3$ was considered in [16], and inspection of (3.2) shows that the techniques used therein adapt readily to all $n \geq 3$. When $\beta < \beta_c = \text{artanh } f_c$, $\mathcal{F}(E)$ vanishes for $E > 0$, and the corrections to $\mathcal{F}_0^{in}(E)$ are small for $E < 0$ with $|E|/M_\star \ll 1$. However, when $\beta > \beta_c$, $\mathcal{F}(E)$ is of the order of M_\star^{n-2} whenever $|E|/M_\star \ll 1$, both for $E > 0$ and for $E < 0$. This is a drastic low energy Lorentz violation, as noted for $n = 3$ in [16].

Suppose then that $n = 2$, in which case (3.2) reduces to

$$\mathcal{F}(E) = \frac{1}{\pi} \int_0^\infty dg |d(g)|^2 \frac{\Theta(g \sinh \beta - |(E/M_\star) + gf(g) \cosh \beta|)}{\sqrt{g^2 \sinh^2 \beta - [(E/M_\star) + gf(g) \cosh \beta]^2}} . \quad (3.5)$$

When $\beta < \beta_c$, $\mathcal{F}(E)$ again vanishes for $E > 0$, and the corrections to $\mathcal{F}_0^{in}(E)$ are small for $E < 0$ with $|E|/M_\star \ll 1$. When $\beta > \beta_c$, $\mathcal{F}(E)$ is nonvanishing and of order unity whenever $|E|/M_\star \ll 1$, and for $E < 0$ it is larger than $\mathcal{F}_0^{in}(E)$ by a factor of order unity. This amounts to a low energy Lorentz violation that is large, in the sense of having a magnitude that is comparable to the Lorentz-invariant de-excitation rate. However, the violation does not involve enhancement factors by positive powers of $M_\star/|E|$ as in $n \geq 3$.

3.2 Graphics for spacetime dimension $2 + 1$

Figures 1 and 2 give plots of the $n = 2$ transition rate $\mathcal{F}(E)$ (3.5), as a function of β and E/M_\star . The plots use the dispersion relation and the density-of-states given by

$$f(g) = \sqrt{(1 - f_c^2)(g - 1)^2 + f_c^2} , \quad (3.6a)$$

$$f_c = 0.8781 , \quad (3.6b)$$

$$d(g) = 1/\sqrt{2f(g)} . \quad (3.6c)$$

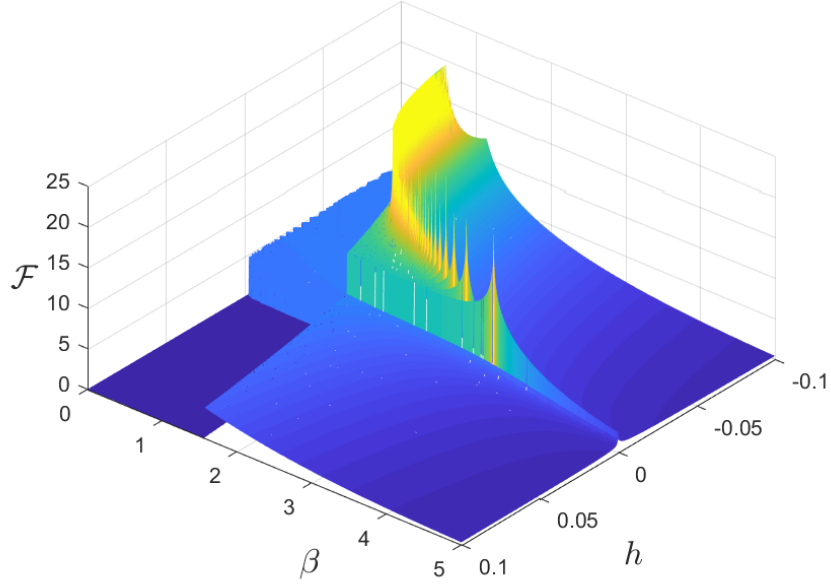


Figure 1: A perspective plot of the $n = 2$ transition rate $\mathcal{F}(E)$ (3.5), as a function of β and $h = E/M_\star$, for the dispersion relation and density of states (3.6). In the low energy regime, $|E|/M_\star \ll 1$, large deviations from the Lorentz-invariant transition rate (3.4) are apparent when β increases above the critical value $\beta_c \approx 1.3675$.

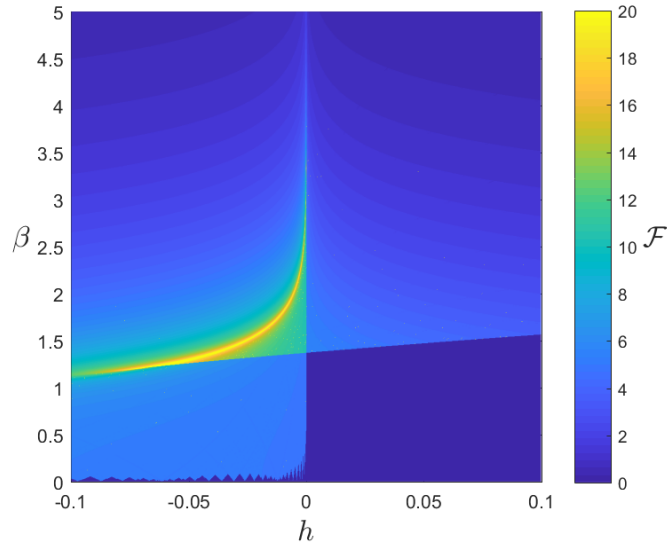


Figure 2: As in Figure 1 but in a topdown colour (grayscale) plot.

We chose this dispersion relation for its numerical amenability and its qualitative similarity to the dispersion relation that emerges from the low energy limit of the polymer quantised scalar field [7, 8, 9].

When $|E|/M_\star \ll 1$, the jump as β increases above $\beta_c \approx 1.3675$ is plain in the plots.

The large spike in the plots at negative E/M_\star is a genuine infinity that occurs along a curve in the $(\beta, E/M_\star)$ plane. (That the perspective plot in Figure 1 shows individual spikes, rather than a curve, is a numerical artefact.) The mathematical reason for this de-excitation resonance is that for values of $(\beta, E/M_\star)$ on this curve, the function of g under the square root in (3.5) has a quadratic minimum at value zero. The spike starts to occur for $\beta \gtrsim 1.2059$, and it exists for $-0.06917 \lesssim E/M_\star < 0$. This de-excitation resonance has no counterpart for $n \geq 3$ because the exponent $(n-3)/2$ in (3.2) is nonnegative for $n \geq 3$.

3.3 Spacetime dimension $1+1$

Finally, we consider spacetime dimension $1+1$, so that $n=1$.

The Wightman function (2.6) is now infrared divergent. However, ignoring this divergence and proceeding formally through steps similar to those in (3.2), we obtain

$$\mathcal{F}(E) = \frac{1}{M_\star} \int_0^\infty \frac{dg}{g} |d(g)|^2 \left[\delta((E/M_\star) + gf(g) \cosh \beta - g \sinh \beta) + \delta((E/M_\star) + gf(g) \cosh \beta + g \sinh \beta) \right], \quad (3.7)$$

from which the infrared divergence has disappeared at the step of interchanging the integrals. Performing the integral in (3.7) gives

$$\mathcal{F}(E) = \sum_j \frac{|d(g_j)|^2}{|E - M_\star g_j^2 f'(g_j)|}, \quad (3.8)$$

where g_j are the solutions to

$$0 = \frac{E}{M_\star} + gf(g) \cosh \beta \mp g \sinh \beta, \quad (3.9)$$

including both signs. The upper (lower) sign in (3.9) comes from the first (second) Dirac delta in (3.7). We adopt (3.7), or equivalently (3.8) and (3.9), as the definition of $\mathcal{F}(E)$. The same answer may be obtained by introducing both an infrared cutoff and a long time cutoff and taking a suitable limit, via a procedure discussed in the context of the Unruh effect in [40].

The transition rate of the Lorentz-invariant massless scalar field is obtained by setting $f(g) = 1$ and $d(g) = 1/\sqrt{2}$ in (3.8) and (3.9), with the outcome

$$\mathcal{F}_0^{in}(E) = \frac{\Theta(-E)}{(-E)}. \quad (3.10)$$

Note that (3.10) fits in the $n \geq 2$ pattern of (3.4), in the sense that setting $n=1$ in (3.4) agrees with (3.10).

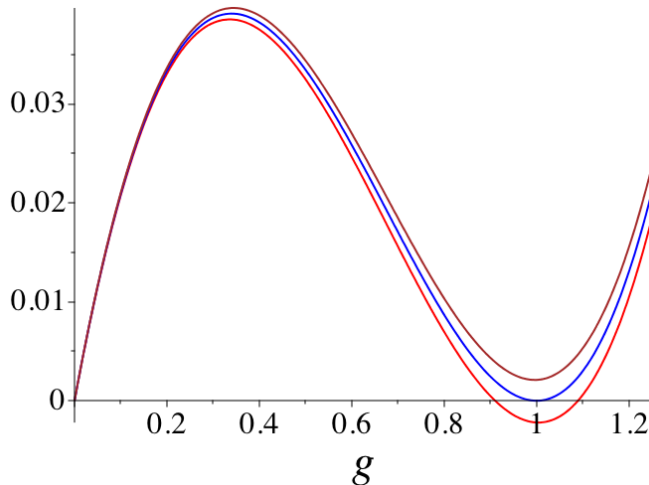


Figure 3: Plot of the function $gf(g) \cosh \beta - g \sinh \beta$, with f given in (3.6). The middle curve is for $\beta = \beta_c \approx 1.3675$, the top curve is for $\beta = 1.363 < \beta_c$, and the bottom curve is for $\beta = 1.372 > \beta_c$.

We wish to compare $\mathcal{F}(E)$ with $\mathcal{F}_0^{in}(E)$ in the low energy limit, $|E|/M_\star \ll 1$.

Suppose first that $\beta < \beta_c$. For $E > 0$, $\mathcal{F}(E)$ vanishes. For $E < 0$, $\mathcal{F}(E)$ tends to $\mathcal{F}_0^{in}(E)$ for sufficiently small $|E|/M_\star$, but the sense of “sufficiently small” depends on β : if β is close to β_c , $\mathcal{F}(E)$ has a divergent peak at the negative value of E for which the argument of the first delta-function in (3.7) has the stationary value zero, and this divergent peak can be made to occur at arbitrarily low $|E|/M_\star$ by taking β close to β_c . We illustrate this phenomenon in Figure 3, where the top curve shows the function $gf(g) \cosh \beta - g \sinh \beta$ with the f given in (3.6) and β slightly below β_c .

Suppose then that $\beta > \beta_c$. The first delta-function in (3.7) brings in additional contributions to $\mathcal{F}(E)$ whenever $|E|/M_\star \ll 1$, regardless the sign of E . These contributions come from g of order unity, and for sufficiently small $|E|/M_\star$ they are of order $1/M_\star$, and hence small compared with $\mathcal{F}_0^{in}(E)$, but the sense of “sufficiently small” again depends on β : if β is close to β_c , $\mathcal{F}(E)$ now has a divergent peak at the positive value of E for which the argument of the first delta-function in (3.7) has the stationary value zero, and this divergent peak can be made to occur at arbitrarily low $|E|/M_\star$ by taking β close to β_c . This phenomenon is illustrated by the bottom curve in Figure 3.

Finally, suppose that β is strictly equal to β_c , as illustrated in the middle curve in Figure 3. For $E > 0$, $\mathcal{F}(E)$ vanishes. For $E < 0$ and $|E|/M_\star \ll 1$, the first delta-function in (3.7) brings in additional contributions from g close to g_c , and using (3.8) and (3.9) we find that these contributions are of order $(-EM_\star)^{-1/2}$, which is small compared with $\mathcal{F}_0^{in}(E)$ by the factor $\sqrt{-E/M_\star}$.

To summarise, these observations show that the low energy Lorentz violation is small, except for a finetuned de-excitation (excitation) peak when β is finetuned to be narrowly below (above) β_c .

As a final remark, we note that if $gf'(g) + f(g)$ is not strictly positive and β is sufficiently small, there are also divergent de-excitation peaks that come from the stationary zeroes of the argument of the second delta-function in (3.7). However, these peaks do

not occur at low energies.

4 Circular motion in 2 + 1 dimensions

In this section we consider a detector in uniform circular motion in spacetime dimension 2 + 1. The worldline is

$$\mathbf{x}(\tau) = (t(\tau), \mathbf{x}(\tau)) = (\gamma\tau, R \cos(\gamma\Omega\tau), R \sin(\gamma\Omega\tau)) , \quad (4.1)$$

where R and Ω are positive parameters satisfying $R\Omega < 1$, and $\gamma = 1/\sqrt{1 - R^2\Omega^2}$. R is the radius of the orbit, and Ω is the angular velocity in the preferred Lorentz frame. The worldline is an orbit of the Killing vector $\partial_t + \Omega(x^1\partial_2 - x^2\partial_1)$, and its scalar proper acceleration is $R\Omega^2\gamma^2$.

Inserting the trajectory (4.1) into (2.5) and (2.6), we obtain

$$\begin{aligned} \mathcal{W}(s, 0) &= \int d^2\mathbf{k} |\rho_{\mathbf{k}}|^2 e^{-i\omega_{\mathbf{k}}\gamma s + iR\{k_1[\cos(\gamma\Omega s) - 1] + k_2 \sin(\gamma\Omega s)\}} \\ &= \int_0^\infty dK K |\rho_K|^2 e^{-i\omega_K\gamma s} \int_0^{2\pi} d\varphi e^{2iRK \sin(\gamma\Omega s/2) \sin(\varphi - \gamma\Omega s/2)} \\ &= 2\pi \int_0^\infty dK K |\rho_K|^2 e^{-i\omega_K\gamma s} J_0(2RK \sin(\gamma\Omega s/2)) \\ &= 2\pi \int_0^\infty dK K |\rho_K|^2 e^{-i\omega_K\gamma s} \sum_{m \in \mathbb{Z}} J_m^2(RK) e^{im\gamma\Omega s} . \end{aligned} \quad (4.2)$$

At the second equality we have written $\mathbf{k} = (K \cos \varphi, K \sin \varphi)$, where $0 \leq K < \infty$ and $0 \leq \varphi < 2\pi$. The third equality uses 10.9.1 in [41], and the fourth equality uses the identity

$$J_0(2a \sin x) = \sum_{m \in \mathbb{Z}} J_m^2(a) e^{2imx} , \quad (4.3)$$

which can be verified using 6.681.6 in [42].

Substituting (4.2) into (2.7), performing the integral over s , using (1.1) and (2.2), and writing $g = K/M_\star$, we find

$$\mathcal{F}(E) = \frac{1}{\gamma} \sum_{m \in \mathbb{Z}} \int_0^\infty dg |d(g)|^2 J_m^2(\tilde{M}g) \delta\left(gf(g) - \frac{1}{\tilde{M}} \left(mv - \frac{\tilde{E}}{\gamma}\right)\right) , \quad (4.4)$$

where $\tilde{M} = RM_\star$, $\tilde{E} = RE$ and $v = R\Omega$. v is the detector's speed in the preferred Lorentz frame, and the dimensionless parameters \tilde{M} and \tilde{E} are respectively M_\star and E expressed in units of $1/R$. Note that $0 < v < 1$.

Recall that by assumption f and d are smooth, f is strictly positive and d is nowhere vanishing, and $f(g) \rightarrow 1$ and $d(g) \rightarrow 1/\sqrt{2}$ as $g \rightarrow 0$. Recall also that by assumption the only stationary point of f is a global minimum at $g = g_c > 0$, and we write $f_c = f(g_c)$, where $0 < f_c < 1$. We then have $f'(g) < 0$ for $0 < g < g_c$ and $f'(g) > 0$ for $g > g_c$.

To proceed, we make two additional assumptions. First, we assume that $gf'(g) +$

$f(g) > 0$ for $g > 0$. It follows that $gf(g)$ is a strictly increasing function of g . Performing the integral in (4.4), we then find

$$\mathcal{F}(E) = \frac{1}{\gamma} \sum_{m=\lceil \tilde{E}/(v\gamma) \rceil}^{\infty} \frac{|d(g_m)|^2}{g_m f'(g_m) + f(g_m)} J_m^2(\tilde{M}g_m) , \quad (4.5)$$

where g_m is the unique solution to

$$gf(g) = \frac{1}{\tilde{M}} \left(mv - \frac{\tilde{E}}{\gamma} \right) . \quad (4.6)$$

Second, we assume that $f(g) > 1$ for sufficiently large g , and that $|d(g)|$ is bounded.

We wish to examine $\mathcal{F}(E)$ in the limit $\tilde{M} \rightarrow \infty$. We find that the limit is qualitatively different for $0 < v < f_c$ and $f_c < v < 1$, as given by the following theorem.

Theorem 4.1. *Under the assumptions stated above:*

(i) *For $0 < v < f_c$, $\mathcal{F}(E) \rightarrow \mathcal{F}_0^{circ}(E)$ as $\tilde{M} \rightarrow \infty$, where*

$$\mathcal{F}_0^{circ}(E) = \frac{1}{2\gamma} \sum_{m=\lceil \tilde{E}/(v\gamma) \rceil}^{\infty} J_m^2(mv - (\tilde{E}/\gamma)) . \quad (4.7)$$

(ii) *For $f_c < v < 1$, $\mathcal{F}(E) \rightarrow \mathcal{F}_0^{circ}(E) + \Delta\mathcal{F}$ as $\tilde{M} \rightarrow \infty$, where*

$$\Delta\mathcal{F} = \frac{1}{\pi\gamma} \int_{g_-}^{g_+} dg \frac{|d(g)|^2}{g \sqrt{v^2 - f^2(g)}} , \quad (4.8)$$

and $g_- \in (0, g_c)$ and $g_+ \in (g_c, \infty)$ are the unique solutions to $f(g) = v$ in the respective intervals.

The proof of Theorem 4.1 is given in the Appendix.

Part (i) of Theorem 4.1 says that the detector sees no low energy Lorentz violation when $v < f_c$: $\mathcal{F}_0^{circ}(E)$ is the response for the usual massless scalar field, as is seen by comparing (4.5) and (4.7). The subscript 0 in \mathcal{F}_0^{circ} indicates the usual massless scalar field and the superscript *circ* indicates the circular trajectory.

Part (ii) of Theorem 4.1 says that the detector sees a low energy Lorentz violation when $v > f_c$: this violation shows up as an increase in the excitation and de-excitation rates. The magnitude of the violation is similar to that which occurs in inertial motion in $2 + 1$ dimensions, found in Section 3.

In Figures 4 and 5 we give plots of $\mathcal{F}(E)$, with the dispersion relation and the density of states given in (3.6), increasing \tilde{M} from 1 to 1000. [We note that (3.6) satisfies the technical assumptions of Theorem 4.1.] The plots show how $\mathcal{F}(E)$ converges to the $\tilde{M} \rightarrow \infty$ limit, given by Theorem 4.1 and displayed in the penultimate plot in Figure 5. Comparison with the unmodified dispersion relation transition rate, given in the last plot in Figure 5, shows plainly the low energy Lorentz violation when v increases above f_c .

Two comments on the numerics are in order. First, when $v > f_c$ and \tilde{M} is large, the Lorentz-breaking contribution to the sum in (4.5) comes from values of m that are

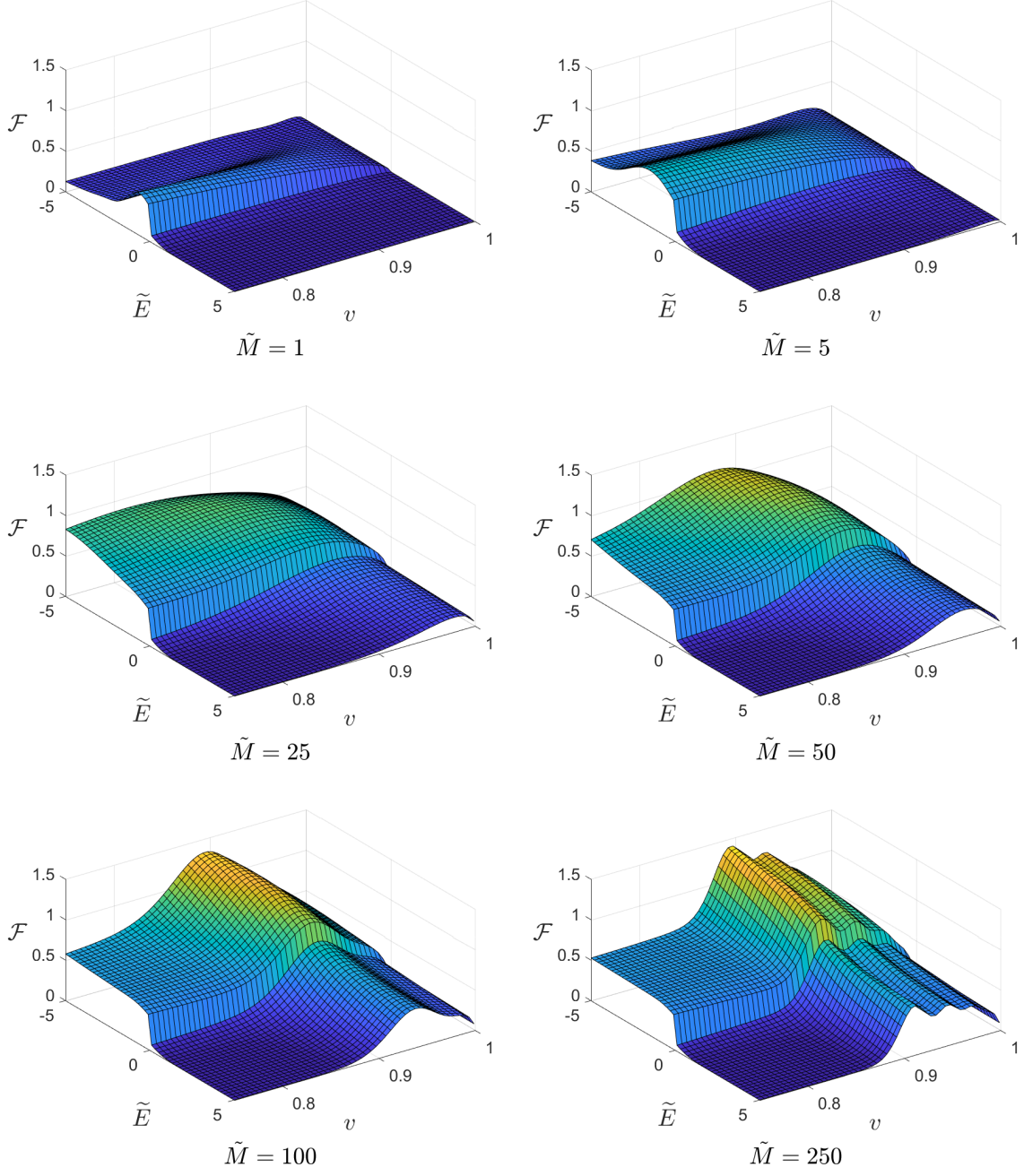


Figure 4: Plots of $\mathcal{F}(E)$ (4.5) as a function of $\tilde{E} = RE$ and v , for f and d given by (3.6), with \tilde{M} increasing from 1 to 250 as shown.

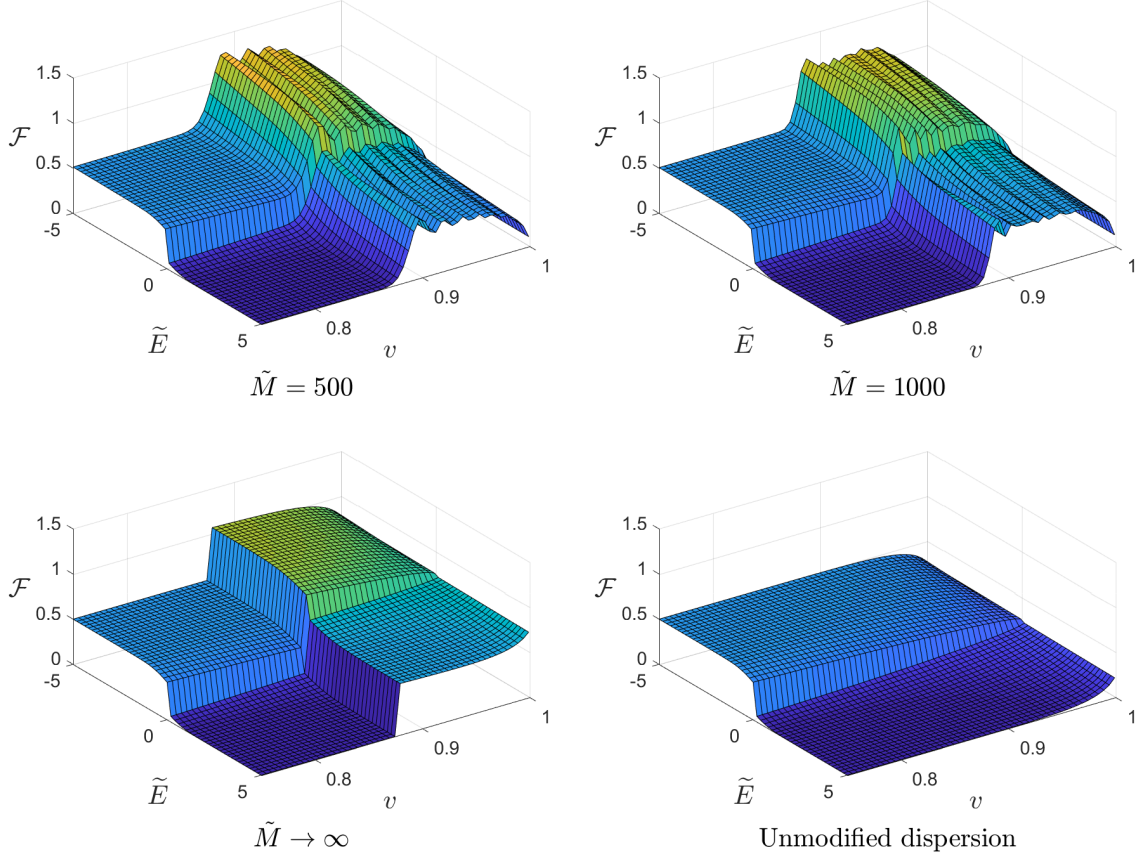


Figure 5: The first two plots continue from Figure 4, with \tilde{M} increasing to 1000. The third plot shows the $\tilde{M} \rightarrow \infty$ limit, given by Theorem 4.1. The last plot shows the transition rate for the ordinary massless scalar field, given by $\mathcal{F}_0^{circ}(E)$ (4.7). For large \tilde{M} , a large low energy deviation from the ordinary massless scalar field transition rate is clear from the plots when v increases above the critical value $f_c = 0.8781$.

comparable to \tilde{M} , as seen from the proof of Part (ii) of Theorem 4.1 in the Appendix. In the numerical evaluation of $\mathcal{F}(E)$ from (4.5), we chose a summation cutoff that is high enough to include these values of m . Second, we implemented the sum in MATLAB, and we checked that the MATLAB routine for evaluating the Bessel functions in this range of m is in agreement with the analytically known asymptotics, given by (A.2) in the Appendix.

In conclusion, a detector in circular motion in the preferred inertial frame sees a large low energy Lorentz violation when its orbital speed exceeds the critical value f_c . This low energy Lorentz violation is quite similar to the one seen by the inertial detector.

5 Circular motion in spacetime dimensions $3 + 1$ and greater

In this section we consider a detector in uniform circular motion in spacetime dimensions $3 + 1$ and greater.

The circular trajectory (4.1) generalises to

$$\mathbf{x}(\tau) = (t(\tau), \mathbf{x}(\tau)) = (\gamma\tau, R \cos(\gamma\Omega\tau), R \sin(\gamma\Omega\tau), 0, 0, \dots) . \quad (5.1)$$

Inserting (5.1) into (2.5) and (2.6), where now $n \geq 3$, we find that (4.2) is replaced by

$$\begin{aligned} \mathcal{W}(s, 0) &= \int d^n \mathbf{k} |\rho_{|\mathbf{k}|}|^2 e^{-i\omega_{|\mathbf{k}|}\gamma s + iR\{k_1[\cos(\gamma\Omega s) - 1] + k_2 \sin(\gamma\Omega s)\}} \\ &= \int d^{n-2} \mathbf{z} \int_0^\infty dL L |\rho_K|^2 e^{-i\omega_K \gamma s} \int_0^{2\pi} d\varphi e^{2iRL \sin(\gamma\Omega s/2) \sin(\varphi - \gamma\Omega s/2)} \\ &= 2\pi \int d^{n-2} \mathbf{z} \int_0^\infty dL L |\rho_K|^2 e^{-i\omega_K \gamma s} J_0(2RL \sin(\gamma\Omega s/2)) \\ &= 2\pi \int d^{n-2} \mathbf{z} \int_0^\infty dL L |\rho_K|^2 e^{-i\omega_K \gamma s} \sum_{m \in \mathbb{Z}} J_m^2(RL) e^{im\gamma\Omega s} , \end{aligned} \quad (5.2)$$

where $K = \sqrt{L^2 + \mathbf{z}^2}$. At the second equality we have written $\mathbf{k} = (L \cos \varphi, L \sin \varphi, z_1, \dots, z_{n-2})$, where $0 \leq L < \infty$ and $0 \leq \varphi < 2\pi$.

We next write \mathbf{z} in $(n - 2)$ -dimensional polar coordinates, so that $Z = |\mathbf{z}| \geq 0$ is the

radius. Integration over the $n - 3$ angles gives the factor Ω_{n-3} , and we obtain

$$\begin{aligned}
\mathcal{W}(s, 0) &= \frac{4\pi^{n/2}}{\Gamma(\frac{n-2}{2})} \int_{\substack{0 \leq Z < \infty \\ 0 \leq L < \infty}} dZ dL Z^{n-3} L |\rho_K|^2 e^{-i\omega_K \gamma s} \sum_{m \in \mathbb{Z}} J_m^2(RL) e^{im\gamma \Omega s} \\
&= \frac{4\pi^{n/2}}{\Gamma(\frac{n-2}{2})} \int_0^\infty dK K^{n-1} |\rho_K|^2 e^{-i\omega_K \gamma s} \\
&\quad \times \sum_{m \in \mathbb{Z}} e^{im\gamma \Omega s} \int_0^{\pi/2} d\alpha \sin \alpha (\cos \alpha)^{n-3} J_m^2(RK \sin \alpha) \\
&= \frac{2}{(4\pi)^{n/2}} \sum_{m \in \mathbb{Z}} \int_0^\infty dK |d(K/M_\star)|^2 \frac{R^{2|m|} K^{2|m|+n-2}}{2^{|m|} \Gamma(|m|+1) \Gamma(|m|+n-\frac{3}{2})} \\
&\quad \times e^{-i(\omega_K - m\Omega)\gamma s} {}_1F_2(|m| + \frac{1}{2}; 2|m| + 1, |m| + n - \frac{3}{2}; -R^2 K^2) , \tag{5.3}
\end{aligned}$$

where ${}_1F_2$ is the generalised hypergeometric function [41]. The second equality in (5.3) comes from writing $(Z, L) = (K \cos \alpha, K \sin \alpha)$ with $0 \leq \alpha \leq \pi/2$. The third equality comes from using the identity

$$\begin{aligned}
&\int_0^{\pi/2} d\alpha \sin \alpha (\cos \alpha)^{n-3} J_\mu^2(z \sin \alpha) \\
&= \frac{z^{2\mu} \Gamma(\frac{n-2}{2})}{2^{2\mu+1} \Gamma(\mu+1) \Gamma(\mu+n-\frac{3}{2})} {}_1F_2(\mu + \frac{1}{2}; 2\mu + 1, \mu + n - \frac{3}{2}; -z^2) , \tag{5.4}
\end{aligned}$$

where $\mu > -1/2$, and the observation that $J_m^2(z) = J_{|m|}^2(z)$ for $m \in \mathbb{Z}$. (5.4) may be verified by using 8.442.1, 3.621.5 and 8.384.1 in [42] and 5.5.5 in [41].

Finally, substituting (5.3) into (2.7), performing the integral over s , using (1.1) and (2.2), and writing $g = K/M_\star$, we have

$$\begin{aligned}
\mathcal{F}(E) &= \frac{M_\star^{n-2}}{(4\pi)^{(n-2)/2} \gamma} \sum_{m \in \mathbb{Z}} \frac{\tilde{M}^{2|m|}}{2^{|m|} \Gamma(|m|+1) \Gamma(|m|+n-\frac{3}{2})} \\
&\quad \times \int_0^\infty dg |d(g)|^2 g^{2|m|+n-2} {}_1F_2(|m| + \frac{1}{2}; 2|m| + 1, |m| + n - \frac{3}{2}; -\tilde{M}^2 g^2) \\
&\quad \times \delta \left(gf(g) - \frac{1}{\tilde{M}} \left(mv - \frac{\tilde{E}}{\gamma} \right) \right) , \tag{5.5}
\end{aligned}$$

where \tilde{M} , \tilde{E} and v are as in (4.4). Assuming that $gf'(g) + f(g) > 0$ for $g > 0$, we may perform the integral over g , finding

$$\begin{aligned}
\mathcal{F}(E) &= \frac{M_\star^{n-2}}{(4\pi)^{(n-2)/2} \gamma} \sum_{m=\lceil \tilde{E}/(v\gamma) \rceil}^\infty \frac{\tilde{M}^{2|m|} |d(g_m)|^2 g_m^{2|m|+n-2}}{2^{|m|} \Gamma(|m|+1) \Gamma(|m|+n-\frac{3}{2}) (g_m f'(g_m) + f(g_m))} \\
&\quad \times {}_1F_2(|m| + \frac{1}{2}; 2|m| + 1, |m| + n - \frac{3}{2}; -\tilde{M}^2 g_m^2) , \tag{5.6}
\end{aligned}$$

where g_m is the unique solution to (4.6).

We would again be interested in $\mathcal{F}(E)$ in the limit $\tilde{M} \rightarrow \infty$. The $(2+1)$ -dimensional results of Section 4 suggest that when $v < f_c$, $\mathcal{F}(E)$ could be expected to tend in this limit to the usual massless scalar field transition rate, given now by

$$\mathcal{F}_0^{circ}(E) = \frac{1}{(4\pi)^{(n-2)/2} \gamma R^{n-2}} \sum_{m=\lceil \tilde{E}/(v\gamma) \rceil}^{\infty} \frac{(mv - \tilde{E}/\gamma)^{2|m|+n-2}}{2^{|m|+1} \Gamma(|m|+1) \Gamma(|m|+n-\frac{3}{2})} \\ \times {}_1F_2\left(|m| + \frac{1}{2}; 2|m|+1, |m|+n-\frac{3}{2}; -(mv - \tilde{E}/\gamma)^2\right), \quad (5.7)$$

whereas when $v > f_c$, we could expect a large additional contribution, providing a low energy Lorentz violation. Unfortunately, we have not been able to investigate these expectations systematically. An analytic investigation would require a uniform asymptotic estimate for the summands in (5.6). A numerical investigation would require an accurate numerical evaluation of the generalised hypergeometric functions in (5.6) and (5.7), including the large values of m that could be expected to bring in the Lorentz-breaking contribution when $v > f_c$.

Circular motion in four spacetime dimensions was investigated in [17]. Equation (25) therein agrees with the $n = 3$ case of our (5.6) when $E \geq 0$, and numerical evidence is presented from the regime $v < f_c$ and $E > 0$, indicating that in this regime $\mathcal{F}(E) \rightarrow \mathcal{F}_0^{circ}(E)$ as $\tilde{M} \rightarrow \infty$. This numerical evidence is consistent with the expectations we have voiced above.

6 Summary and discussion

We have investigated the low energy phenomenology of a relativistic scalar field that violates Lorentz invariance at high energies, by coupling the field to an inertial Unruh-DeWitt detector in Minkowski spacetimes of dimension two or greater, and to an Unruh-DeWitt detector in uniform circular motion in Minkowski spacetimes of dimension three or greater. The dispersion relation was assumed to be Lorentz invariant at low energies but subluminal in some interval of high energies. We showed that the inertial detector experiences a large Lorentz violation at low energies in all spacetime dimensions greater than two when the detector's velocity in the preferred frame exceeds a critical velocity determined by the dispersion relation: this generalises results obtained previously in four dimensions in [15, 16]. We also showed that a similar large low energy Lorentz violation occurs for a detector in circular motion in $2+1$ dimensions. Finally, we laid the analytic groundwork for examining circular motion in all dimensions greater than $2+1$, generalising the $(3+1)$ -dimensional analysis of [17].

On the theoretical side, our analysis was motivated by the high energy Lorentz violations that occur in many approaches to quantum gravity, and the hope to constrain these violations by low energy phenomenology. For example, as discussed in [16], the four-dimensional inertial motion results appear to experimentally rule out a field quantised in the polymer quantisation framework [4, 5, 6, 7, 8, 9] that is motivated by loop quantum gravity [10, 11], in the implementation of this framework adopted in [7].

On a more practical side, we anticipate that our results may be applicable to analogue

spacetime laboratory experiments, where the effective spacetime dimension often differs from four [18, 19, 20, 21, 22]. We leave the development of this topic as a subject of future work.

Acknowledgments

We thank Antonin Coutant, Cisco Gooding, Viqar Husain, Sanjeev Seahra, Lakshmanan Sriramkumar, Silke Weinfurtner and L. J. Zhou for helpful discussions and correspondence. JL was supported in part by Science and Technology Facilities Council (Theory Consolidated Grants ST/J000388/1 and ST/P000703/1). SDU was supported by a summer research bursary from the School of Mathematical Sciences, University of Nottingham.

A Appendix: Proof of Theorem 4.1

In this appendix we give the proof of Theorem 4.1.

A.1 Case (i): $0 < v < f_c$

Suppose that $0 < v < f_c$.

From (4.6) we see that $\tilde{M}g_m \rightarrow mv - \tilde{E}/\gamma$ as $\tilde{M} \rightarrow \infty$, for each fixed m . From 10.14.2 and 10.14.7 in [41] it follows that for sufficiently large \tilde{M} there exist constants $m_0 \in \mathbb{Z}_+$, $\alpha > 0$ and $C > 0$, independent of \tilde{M} , such that $0 < J_m(\tilde{M}g_m) < Cm^{-1/3}e^{-\alpha m}$ for all $m \geq m_0$. Since $|d(g)|$ and $(gf'(g) + f(g))^{-1}$ are bounded under our assumptions, it follows by a dominated convergence argument that the $\tilde{M} \rightarrow \infty$ limit in (4.5) can be taken under the sum. This completes the proof of Case (i).

A.2 Case (ii): $f_c < v < 1$

Suppose that $f_c < v < 1$. Recall that under our assumptions the equation $f(g) = v$ then has exactly two solutions, denoted by $g_- \in (0, g_c)$ and $g_+ \in (g_c, \infty)$.

To begin, we choose constants $g_1 \in (0, g_-)$ and $g_2 \in (g_+, \infty)$. Note that $v < f(g_1) < 1$ and $v < f(g_2)$. For sufficiently large \tilde{M} , the set of integers m for which $g_m \in (0, g_1)$ is nonempty and bounded from above, and we denote the largest integer in this set by m_1 . Similarly, the set of integers m for which $g_m \in (g_2, \infty)$ is nonempty and bounded from below, and we denote the smallest integer in this set by m_2 . Note that m_1 and m_2 depend on \tilde{M} , they satisfy $m_1 < m_2$, and they both tend to infinity as $\tilde{M} \rightarrow \infty$.

Let \tilde{M} now be so large that $m_1 > \max(1, 1 + \lceil \tilde{E}/(v\gamma) \rceil)$. Let $\mathcal{F}_1(E)$, $\mathcal{F}_2(E)$ and $\mathcal{F}_3(E)$ be the contributions to $\mathcal{F}(E)$ (4.5) from respectively $m < m_1$, $m_1 \leq m \leq m_2$ and $m > m_2$. We need to estimate each of $\mathcal{F}_1(E)$, $\mathcal{F}_2(E)$ and $\mathcal{F}_3(E)$.

In $\mathcal{F}_1(E)$ and $\mathcal{F}_3(E)$, 10.14.2 and 10.14.7 in [41] again provide a dominated convergence bound that justifies taking the $\tilde{M} \rightarrow \infty$ limit under the sum over m . The outcome is that $\mathcal{F}_1(E) \rightarrow \mathcal{F}_0^{\text{circ}}(E)$ and $\mathcal{F}_3(E) \rightarrow 0$ as $\tilde{M} \rightarrow \infty$.

In $\mathcal{F}_2(E)$, we view the sum over m as the Riemann sum for an integral in the variable m/\tilde{M} . Changing the integration variable from m/\tilde{M} to g by (4.6) shows that

the $\tilde{M} \rightarrow \infty$ limit of $\mathcal{F}_2(E)$ is given by the $\tilde{M} \rightarrow \infty$ limit of

$$\tilde{\mathcal{F}}_{\tilde{M}}(E) = \frac{1}{v\gamma} \int_{g_1}^{g_2} dg |d(g)|^2 \tilde{M} J_{\frac{\tilde{M}}{v}}^2 \left(gf(g) + \frac{\tilde{E}}{\gamma \tilde{M}} \right) (\tilde{M}g) , \quad (\text{A.1})$$

provided the $\tilde{M} \rightarrow \infty$ limit of the integrand in (A.1) exists and is sufficiently uniform in g . That the limit has these properties under our assumptions follows from the uniform asymptotic expansion of $J_\nu(\nu z)$ as $\nu \rightarrow \infty$, given by 10.20.4 in [41], together with the asymptotic expansions of the Airy function Ai at large positive and negative argument, given by 9.7.5 and 9.7.9 in [41]. The key property responsible for a nonvanishing answer in the limit is that

$$\nu J_\nu^2(\nu z) = \frac{2}{\pi \sqrt{z^2 - 1}} \cos^2 \left[\nu \left(\sqrt{z^2 - 1} - \text{arccsc } z \right) - \frac{\pi}{4} \right] + o(1) \quad (\text{A.2})$$

as $\nu \rightarrow \infty$ with fixed $z > 1$, together with an appropriate uniformity discussion in (A.2), and the use of the identity $2 \cos^2 z = 1 + \cos(2z)$ and the Riemann-Lebesgue lemma to justify the replacement $2 \cos^2 \rightarrow 1$ when (A.2) is used under the integral in (A.1). We find that $\mathcal{F}_2(E) \rightarrow \Delta \mathcal{F}$ as $\tilde{M} \rightarrow \infty$, where $\Delta \mathcal{F}$ is given by (4.8).

This completes the proof of Case (ii). ■

References

- [1] G. Amelino-Camelia, “Quantum-Spacetime Phenomenology,” *Living Rev. Rel.* **16**, 5 (2013) [arXiv:0806.0339 [gr-qc]].
- [2] J. Collins, A. Perez, D. Sudarsky, L. Urrutia and H. Vucetich, “Lorentz invariance and quantum gravity: an additional fine-tuning problem?,” *Phys. Rev. Lett.* **93**, 191301 (2004) [gr-qc/0403053].
- [3] J. Polchinski, “Comment on [arXiv:1106.1417] ‘Small Lorentz violations in quantum gravity: do they lead to unacceptably large effects?’,” *Class. Quant. Grav.* **29**, 088001 (2012) [arXiv:1106.6346 [gr-qc]].
- [4] A. Ashtekar, S. Fairhurst and J. L. Willis, “Quantum gravity, shadow states, and quantum mechanics,” *Class. Quant. Grav.* **20**, 1031 (2003) [arXiv:gr-qc/0207106].
- [5] A. Ashtekar, J. Lewandowski and H. Sahlmann, “Polymer and Fock representations for a scalar field,” *Class. Quant. Grav.* **20**, L11 (2003) [arXiv:gr-qc/0211012].
- [6] V. Husain and A. Kreienbuehl, “Ultraviolet behavior in background independent quantum field theory,” *Phys. Rev. D* **81**, 084043 (2010) [arXiv:1002.0138 [gr-qc]].
- [7] G. M. Hossain, V. Husain and S. S. Seahra, “Propagator in polymer quantum field theory,” *Phys. Rev. D* **82**, 124032 (2010) [arXiv:1007.5500 [gr-qc]].
- [8] G. M. Hossain, V. Husain and S. S. Seahra, “Non-singular inflationary universe from polymer matter,” *Phys. Rev. D* **81**, 024005 (2010) [arXiv:0906.2798 [astro-ph.CO]].

- [9] S. S. Seahra, I. A. Brown, G. M. Hossain and V. Husain, “Primordial polymer perturbations,” JCAP **1210**, 041 (2012) [arXiv:1207.6714 [astro-ph.CO]].
- [10] C. Rovelli, *Quantum Gravity* (Cambridge University Press, Cambridge, 2007).
- [11] T. Thiemann, *Modern Canonical Quantum General Relativity* (Cambridge University Press, Cambridge, 2008).
- [12] D. Vollhardt and P. Wölfle, *The Superfluid Phases of Helium 3* (Taylor and Francis, London, 1990).
- [13] W. G. Unruh, “Notes on black hole evaporation,” Phys. Rev. D **14**, 870 (1976).
- [14] B. S. DeWitt, “Quantum gravity: the new synthesis”, in *General Relativity: an Einstein centenary survey*, edited by S. W. Hawking and W. Israel (Cambridge University Press, Cambridge, 1979).
- [15] N. Kajuri, “Polymer quantization predicts radiation in inertial frames,” Class. Quant. Grav. **33**, 055007 (2016) [arXiv:1508.00659 [gr-qc]].
- [16] V. Husain and J. Louko, “Low energy Lorentz violation from modified dispersion at high energies,” Phys. Rev. Lett. **116**, 061301 (2016) [arXiv:1508.05338 [gr-qc]].
- [17] D. J. Stargen, N. Kajuri and L. Sriramkumar, “Response of a rotating detector coupled to a polymer quantized field,” Phys. Rev. D **96**, 066002 (2017) [arXiv:1706.05834 [gr-qc]].
- [18] F. Belgiorno *et al.*, “Hawking radiation from ultrashort laser pulse filaments,” Phys. Rev. Lett. **105**, 203901 (2010) [arXiv:1009.4634 [gr-qc]].
- [19] S. Weinfurtner, E. W. Tedford, M. C. J. Penrice, W. G. Unruh and G. A. Lawrence, “Measurement of stimulated Hawking emission in an analogue system,” Phys. Rev. Lett. **106**, 021302 (2011) [arXiv:1008.1911 [gr-qc]].
- [20] J. Steinhauer, “Observation of quantum Hawking radiation and its entanglement in an analogue black hole,” Nature Phys. **12**, 959 (2016) [arXiv:1510.00621 [gr-qc]].
- [21] T. Torres, S. Patrick, A. Coutant, M. Richartz, E. W. Tedford and S. Weinfurtner, “Rotational superradiant scattering in a vortex flow,” Nature Phys. **13**, 833 (2017) [arXiv:1612.06180 [gr-qc]].
- [22] U. Leonhardt, I. Griniasty, S. Wildeman, E. Fort and M. Fink, “Classical analogue of the Unruh effect,” arXiv:1709.02200 [gr-qc].
- [23] J. S. Bell and J. M. Leinaas, “Electrons as accelerated thermometers,” Nucl. Phys. B **212**, 131 (1983).
- [24] J. S. Bell and J. M. Leinaas, “The Unruh effect and quantum fluctuations of electrons in storage rings,” Nucl. Phys. B **284**, 488 (1987).

- [25] J. M. Leinaas, “Accelerated electrons and the Unruh effect,” in *Quantum aspects of beam physics. Proceedings, Advanced ICFA Beam Dynamics Workshop, Monterey, USA, January 4-9, 1998*, edited by P. Chen (World Scientific, Singapore, 1999).
- [26] W. G. Unruh, “Acceleration radiation for orbiting electrons,” *Phys. Rept.* **307**, 163 (1998) [arXiv:hep-th/9804158].
- [27] A. Retzker, J. I. Cirac, M. B. Plenio and B. Reznik, “Methods for detecting acceleration radiation in a Bose-Einstein condensate,” *Phys. Rev. Lett.* **101**, 110402 (2008) [arXiv:0709.2425 [quant-ph]].
- [28] Y. Jin, J. Hu and H. Yu, “Spontaneous excitation of a circularly accelerated atom coupled to electromagnetic vacuum fluctuations,” *Annals Phys.* **344**, 97 (2014).
- [29] Y. Jin, J. Hu and H. Yu, “Dynamical behavior and geometric phase for a circularly accelerated two-level atom,” *Phys. Rev. A* **89**, 064101 (2014) [arXiv:1406.5576 [gr-qc]].
- [30] E. Martín-Martínez, M. Montero and M. del Rey, “Wavepacket detection with the Unruh-DeWitt model,” *Phys. Rev. D* **87**, 064038 (2013) [arXiv:1207.3248 [quant-ph]].
- [31] Á. M. Alhambra, A. Kempf and E. Martín-Martínez, “Casimir forces on atoms in optical cavities,” *Phys. Rev. A* **89**, 033835 (2014) [arXiv:1311.7619 [quant-ph]].
- [32] N. D. Birrell and P. C. W. Davies, *Quantum Fields in Curved Space* (Cambridge University Press, Cambridge, 1982).
- [33] R. M. Wald, *Quantum field theory in curved spacetime and black hole thermodynamics* (University of Chicago Press, Chicago, USA, 1994).
- [34] L. C. B. Crispino, A. Higuchi and G. E. A. Matsas, “The Unruh effect and its applications,” *Rev. Mod. Phys.* **80**, 787 (2008) [arXiv:0710.5373 [gr-qc]].
- [35] B. L. Hu, S. Y. Lin and J. Louko, “Relativistic quantum information in detectors-field interactions,” *Class. Quant. Grav.* **29**, 224005 (2012) [arXiv:1205.1328 [quant-ph]].
- [36] E. Martín-Martínez and N. C. Menicucci, “Entanglement in curved spacetimes and cosmology,” *Class. Quant. Grav.* **31**, no. 21, 214001 (2014) [arXiv:1408.3420 [quant-ph]].
- [37] A. Satz, “Then again, how often does the Unruh-DeWitt detector click if we switch it carefully?,” *Class. Quant. Grav.* **24**, 1719 (2007) [arXiv:gr-qc/0611067].
- [38] J. Louko and A. Satz, “Transition rate of the Unruh-DeWitt detector in curved spacetime,” *Class. Quant. Grav.* **25**, 055012 (2008) [arXiv:0710.5671 [gr-qc]].
- [39] C. J. Fewster, B. A. Juárez-Aubry and J. Louko, “Waiting for Unruh,” *Class. Quant. Grav.* **33**, 165003 (2016) [arXiv:1605.01316 [gr-qc]].

- [40] S. Takagi, “Vacuum noise and stress induced by uniform acceleration: Hawking-Unruh effect in Rindler manifold of arbitrary dimension,” *Prog. Theor. Phys. Suppl.* **88**, 1 (1986).
- [41] *NIST Digital Library of Mathematical Functions*, <http://dlmf.nist.gov/>, Release 1.0.15 of 2017-06-01. F. W. J. Olver, A. B. Olde Daalhuis, D. W. Lozier, B. I. Schneider, R. F. Boisvert, C. W. Clark, B. R. Miller, and B. V. Saunders, eds.
- [42] I. S. Gradshteyn and I. M. Ryzhik, *Table of Integrals, Series, and Products*, 7th edition (Academic Press, New York, 2007).